

Electronic Supplementary Information

A carbene stabilized precursor for the spatial atomic layer deposition of copper thin films

Nils Boysen^a, Bujamin Misimi^b, Arbresha Muriqi,^c Jan-Lucas Wree^a, Tim Hasselmann^b, Detlef Rogalla^d, Tobias Haeger^b, Detlef Theirich^b, Michael Nolan,^e Thomas Riedl^{b*} and Anjana Devi^{a*}

^a *Inorganic Materials Chemistry, Ruhr University Bochum, 44801 Bochum, Germany (anjana.devi@rub.de)*

^b *Institute of Electronic Devices, University of Wuppertal, 42119 Wuppertal, Germany (t.riedl@uni-wuppertal.de)*

^c *Tyndall National Institute, University College Cork, Lee Maltings, Dyke Parade, Cork T12 R5CP, Ireland*

^d *RUBION, Ruhr University Bochum, 44801 Bochum, Germany*

^e *Tyndall National Institute, University College Cork, Lee Maltings, Dyke Parade, Cork T12 R5CP, Ireland and Nanotechnology and Integrated Bioengineering Centre, Ulster University, Shore Road, Co Antrim, BT37 OQB, Northern Ireland*

S1. General Experimental Considerations

The synthesis and handling of all reagents and products was carried out by standard *Schlenk* protocols using Ar as an inert gas to prevent contact with ambient air. The products of all reactions were stored and handled inside an MBraun 300 Glovebox system. The solvents were dried by an MBraun solvent purification system (SPS) and stored under inert gas atmosphere. All commercially available reagents were used without further purification. NMR measurements were performed on a Bruker Avance III 400 spectrometer in *J. Young* NMR tubes under inert atmosphere. The deuterated NMR solvents were dried *via* the freeze-pump-thaw method and stored over activated molecular sieves prior to use. EA measurements (CHNS) were performed on a Vario Micro Cube from Elementar Analysensysteme GmbH and the samples were prepared in sealed tin crucibles inside a glovebox. Thermogravimetric analysis (TGA) was carried out with a Seiko Exstar TG/DTA 6500SII by employing a constant nitrogen flow (300 ml/min) and a constant heating rate (5 K/min). For each measurement, approx. 10 mg of each compound was used. Single crystals of [Cu(^tBuNHC)(hmds)] were crystallized from hexane at -35 °C. A suitable crystal was selected and mounted on a SuperNova, Atlas diffractometer. The crystal was kept at 100.00(10) K during data collection. Using Olex2,¹ the structure was solved with the SHELXT structure solution program using Intrinsic Phasing and refined with the SHELXL refinement package using Least Squares minimization.^{2,3} CCDC deposition number for [Cu(^tBuNHC)(hmds)]: 2006567.

S2. Synthetic Procedure

Synthesis of [Cu(^tBuNHC)(hmds)]:

1,3-di-*tert*-butyl imidazolium chloride (7.50 g, 34.3 mmol), copper(I) chloride (3.39 g, 34.3 mmol) and [Li(hmds)OEt₂]₂ (16.6 g, 68.6 mmol) were placed together in a *Schlenk* flask under inert atmosphere after which 100 ml of THF were added, heated to reflux. The solvent was removed, and the residual solid was extracted in hexane, reduced under vacuum and [Cu(^tBuNHC)(hmds)] crystallized as colorless crystalline needles. Yield: 11.8 g (84 %). M.p.: 93 °C. ¹H NMR (400 MHz, C₆D₆): δ(ppm) = 2.59 (s, 4H; N(C₂H₄)N), 1.33 (s, 18H; ^{NHC}NC(CH₃)₃), 0.56 (s, 17H; NSi(CH₃)₃). ¹³C NMR (101 MHz, C₆D₆): δ(ppm) = 201.58 (^{NHC}NCN), 55.10 (N(C₂H₄)N), 45.29 (^{NHC}NC(CH₃)₃), 30.84 (^{NHC}NC(CH₃)₃), 6.91 (NSi(CH₃)₃). Elemental Analysis: Calc.: C, 50.26; H, 9.93; N, 10.34; Meas. C, 48.92; H, 8.68; N, 10.70. Crystal Data for [Cu(^tBuNHC)(hmds)] (*M*=406.24 g/mol): triclinic, space group P $\bar{1}$ (no. 2), *a* = 8.8580(5) Å, *b* = 9.6854(6) Å, *c* = 14.7645(9) Å, α = 104.257(5)°, β = 103.276(5)°, γ = 101.697(5)°, *V* = 1148.84(13) Å³, *Z* = 2, *T* = 100.00(10) K, μ (Cu K α) = 2.347 mm⁻¹, *D*_{calc} = 1.174 g/cm³, 7922 reflections measured (9.8° ≤ 2 Θ ≤ 146.29°), 4445 unique (*R*_{int} = 0.0248, *R*_{sigma} = 0.0379) which were used in all calculations. The final *R*₁ was 0.0327 (*I* > 2 σ (*I*)) and *wR*₂ was 0.0856 (all data).

S3. Known Copper PEALD Processes

Table S1. A selected summary of known Copper ALD processes and precursors with the focus on plasma-assisted ALD processes.

Cu Precursor	Co-Reactant	T _{dep} (°C)	GPC (Å)	Substrate	Reference
[CuCl]	H ₂	375 – 475	0.8	SiO ₂	Mårtensson et al. ⁴ (1997)
[Cu(acac) ₂]	Ar/H ₂ plasma	200	0.18	Si	Niskanen et al. ⁵ (2005)
[Cu(acac) ₂]	H ₂ plasma	85 – 135	0.2	SiO ₂	Wu et al. ⁶ (2007)
[Cu(thd) ₂]	H ₂ plasma	90 – 250	0.11	SiO ₂	Jezewski et al. ⁷ (2005)
[Cu(maboc) ₂]	H ₂ plasma	100 – 180	0.65	Ta	Moon et al. ⁸ (2011)
[Cu(ⁱ Pr ₃ amd)] ₂	H ₂ plasma	50 – 100	0.71	Si	Guo et al. ⁹ (2015)
[Cu(ⁱ PrNHC)(hmds)]	Ar/H ₂ plasma	225	0.2	Si	Coyle et al. ¹⁰ (2013)
[Cu(^t BuNHC)(hmds)]	Ar/H ₂ plasma*	100	0.23	BSiG**	This work

* spatial process at atmospheric pressure; **BSiG = Borosilicate glass

S4. NMR Spectra of $[\text{Cu}(\text{tBuNHC})(\text{hmds})]$

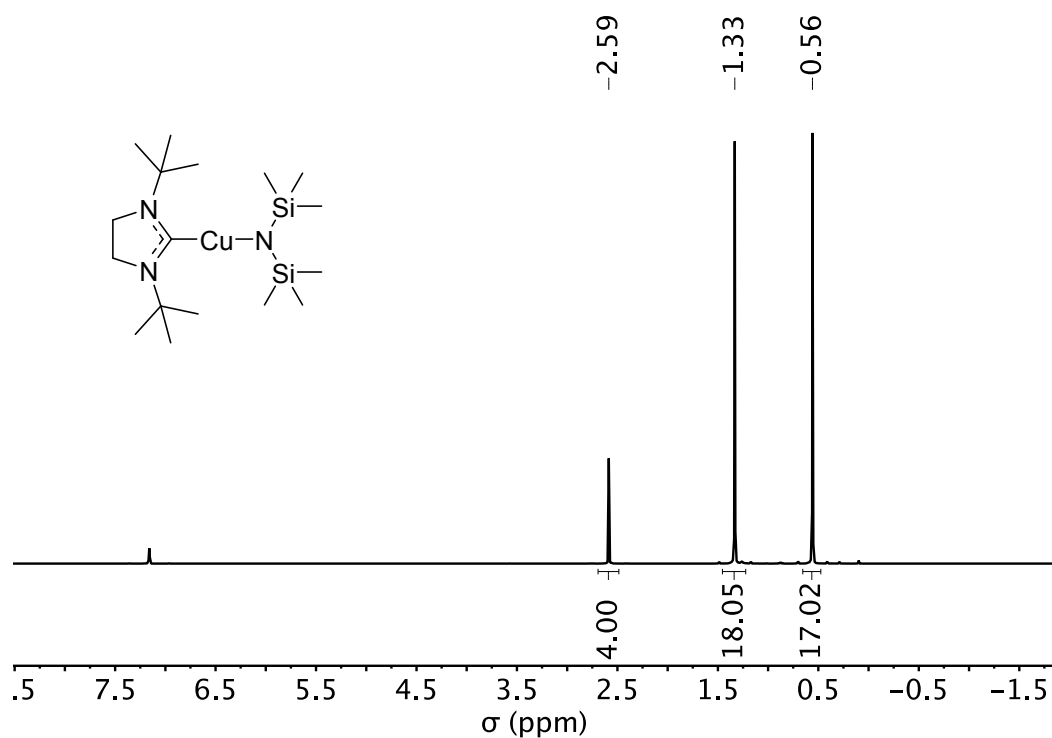


Figure S 1. ^1H NMR spectrum of $[\text{Cu}(\text{tBuNHC})(\text{hmds})]$ measured at 400 MHz and 300 K in C_6D_6 .

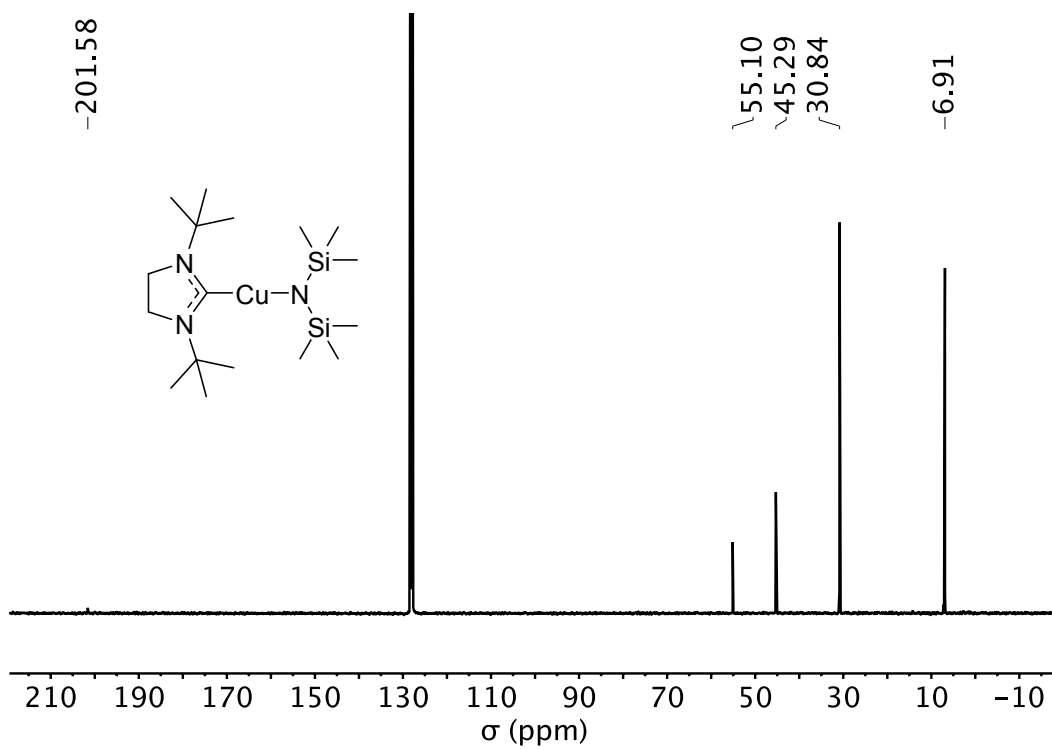


Figure S 2. ^{13}C NMR spectrum of $[\text{Cu}(\text{tBuNHC})(\text{hmds})]$ measured at 101 MHz and 300 K in C_6D_6 .

S5. Crystallographic details of [Cu(^tBuNHC)(hmds)]

Table S2. Crystal data and structure refinement for [Cu(^tBuNHC)(hmds)].

Identification code	[Cu(^t BuNHC)(hmds)]
Empirical formula	C ₁₇ H ₄₀ CuN ₃ Si ₂
Formula weight	406.24
Temperature/K	100.00(10)
Crystal system	triclinic
Space group	$P\bar{1}$
a/Å	8.8580(5)
b/Å	9.6854(6)
c/Å	14.7645(9)
α /°	104.257(5)
β /°	103.276(5)
γ /°	101.697(5)
Volume/Å ³	1148.84(13)
Z	2
$\rho_{\text{calc}}/\text{cm}^3$	1.174
μ/mm^{-1}	2.347
F(000)	440.0
Crystal size/mm ³	0.208 × 0.136 × 0.108
Radiation	Cu K α (λ = 1.54184)
2 Θ range for data collection/°	9.8 to 146.29
Index ranges	-10 ≤ h ≤ 7, -11 ≤ k ≤ 11, -18 ≤ l ≤ 18
Reflections collected	7922
Independent reflections	4445 [R_{int} = 0.0248, R_{sigma} = 0.0379]
Data/restraints/parameters	4445/0/220
Goodness-of-fit on F ²	1.036
Final R indexes [$I \geq 2\sigma(I)$]	$R_1 = 0.0327$, $wR_2 = 0.0805$
Final R indexes [all data]	$R_1 = 0.0400$, $wR_2 = 0.0856$
Largest diff. peak/hole / e Å ⁻³	0.38/-0.29

Table S3. Fractional atomic coordinates ($\times 10^4$) and equivalent isotropic displacement parameters ($\text{\AA}^2 \times 10^3$) for [Cu(^tBuNHC)(hmds)]. U_{eq} is defined as 1/3 of the trace of the orthogonalised U_{ij} tensor.

Atom	x	y	z	U(eq)
Cu01	3460.3(3)	6212.4(3)	2819.3(2)	20.41(9)
Si02	1858.2(6)	3052.7(5)	1556.1(4)	21.10(12)
Si03	-96.3(6)	4817.0(5)	2542.9(4)	21.39(12)
N004	6273.5(18)	8521.1(17)	4187.6(12)	22.2(3)
N005	5900.7(18)	8550.6(16)	2676.1(12)	20.8(3)
N006	1665.6(18)	4562.5(16)	2349.8(12)	20.9(3)
C007	5310(2)	7869.0(19)	3260.2(13)	19.7(3)
C008	5098(2)	8240(2)	1615.2(14)	22.8(4)
C009	7777(2)	9549(2)	4221.5(15)	25.5(4)

C00A	7320(2)	9818(2)	3235.0(15)	27.3(4)
C00B	6209(2)	7895(2)	5008.6(14)	25.4(4)
C00C	5096(3)	6682(2)	1068.4(15)	28.3(4)
C00D	3382(2)	8403(3)	1464.8(16)	30.6(4)
C00E	4499(3)	7578(2)	5094.1(15)	29.1(4)
C00F	3976(2)	2884(2)	1923.3(18)	31.9(4)
C00G	469(2)	1252(2)	1492.5(16)	29.7(4)
C00H	6042(3)	9346(2)	1222.8(16)	32.7(4)
C00I	1408(3)	3117(2)	261.0(15)	31.6(4)
C00J	-1853(2)	4031(3)	1397.8(16)	31.2(4)
C00K	-679(3)	3939(3)	3461.0(17)	36.2(5)
C00L	6768(3)	6483(3)	4835.9(18)	36.4(5)
C00M	7(3)	6836(3)	3009(2)	43.8(6)
C00N	7315(3)	9050(3)	5962.8(16)	41.3(5)

Table S4. Anisotropic displacement parameters ($\text{\AA}^2 \times 10^3$) for $[\text{Cu}(\text{tBuNHC})(\text{hmds})]$. The Anisotropic displacement factor exponent takes the form: $-2\pi^2[h^2a^*U_{11}+2hka^*b^*U_{12}+\dots]$.

Atom	U_{11}	U_{22}	U_{33}	U_{23}	U_{13}	U_{12}
Cu01	17.34(14)	17.25(14)	22.92(15)	5.80(11)	4.68(10)	-1.4(1)
Si02	18.4(2)	16.6(2)	26.8(3)	5.39(19)	8.24(19)	1.43(18)
Si03	17.9(2)	19.5(2)	25.2(3)	5.19(19)	8.15(19)	1.83(18)
N004	19.2(7)	19.3(7)	24.5(8)	6.4(6)	4.5(6)	0.1(6)
N005	17.7(7)	17.2(7)	23.9(8)	6.0(6)	4.7(6)	-0.6(6)
N006	16.3(7)	15.8(7)	25.0(8)	2.6(6)	4.8(6)	-1.3(5)
C007	17.8(8)	15.9(8)	24.8(9)	6.1(7)	6.0(7)	4.1(6)
C008	20.3(9)	23.6(9)	24.6(9)	9.4(7)	7.3(7)	3.4(7)
C009	18.7(9)	22.8(9)	28.6(10)	3.6(8)	5.4(7)	-1.0(7)
C00A	23.0(9)	22.8(9)	28.9(10)	5.1(8)	6.3(8)	-4.2(7)
C00B	26.1(9)	23.7(9)	23.2(9)	8.0(7)	4.4(7)	2.2(7)
C00C	34.1(10)	25.9(9)	24.8(9)	7.6(8)	10.0(8)	6.8(8)
C00D	25.9(10)	40.8(11)	28.7(10)	15.0(9)	7.7(8)	12.2(9)
C00E	32.0(10)	30.5(10)	27.3(10)	12.0(8)	10.8(8)	7.5(8)
C00F	26.6(10)	26.1(10)	46.1(12)	13.9(9)	14.1(9)	6.2(8)
C00G	27.7(10)	18.6(9)	39.2(11)	6.0(8)	11.2(9)	0.3(7)
C00H	35.5(11)	30.7(10)	33.6(11)	16.4(9)	12.3(9)	1.9(8)
C00I	31.5(10)	31.4(10)	28.3(10)	5.7(8)	11.7(8)	1.9(8)
C00J	22.2(9)	39.8(11)	30.7(10)	10.1(9)	6.4(8)	8.9(8)
C00K	32.6(11)	48.7(13)	35.0(11)	18.7(10)	17.5(9)	12.2(10)
C00L	39.4(12)	37.1(12)	43.7(13)	22.6(10)	14.9(10)	18.5(10)
C00M	36.0(12)	26.4(11)	66.6(17)	3.2(11)	23.6(12)	7.7(9)
C00N	43.7(13)	40.2(12)	26.1(11)	9.9(9)	-0.3(9)	-6.1(10)

Table S5. Bond lengths for $[\text{Cu}(\text{tBuNHC})(\text{hmds})]$.

Atom	Atom	Length/ \AA	Atom	Atom	Length/ \AA
Cu01	N006	1.8653(15)	N004	C00B	1.490(2)

Cu01	C007	1.9009(18)	N005	C007	1.342(2)
Si02	N006	1.6999(16)	N005	C008	1.490(2)
Si02	C00F	1.881(2)	N005	C00A	1.472(2)
Si02	C00G	1.8870(19)	C008	C00C	1.525(3)
Si02	C00I	1.881(2)	C008	C00D	1.531(3)
Si03	N006	1.7040(15)	C008	C00H	1.533(3)
Si03	C00J	1.881(2)	C009	C00A	1.521(3)
Si03	C00K	1.881(2)	C00B	C00E	1.524(3)
Si03	C00M	1.882(2)	C00B	C00L	1.530(3)
N004	C007	1.349(2)	C00B	C00N	1.530(3)
N004	C009	1.475(2)			

Table S6. Bond angles for [Cu(^tBuNHC)(hmds)].

Atom	Atom	Atom	Angle/°	Atom	Atom	Atom	Angle/°
N006	Cu01	C007	178.09(7)	Si02	N006	Si03	125.68(9)
N006	Si02	C00F	110.44(9)	Si03	N006	Cu01	117.61(8)
N006	Si02	C00G	113.55(8)	N004	C007	Cu01	126.62(13)
N006	Si02	C00I	113.18(9)	N005	C007	Cu01	124.56(14)
C00F	Si02	C00G	106.84(9)	N005	C007	N004	108.78(15)
C00I	Si02	C00F	107.14(10)	N005	C008	C00C	108.70(15)
C00I	Si02	C00G	105.24(10)	N005	C008	C00D	109.80(15)
N006	Si03	C00J	112.92(9)	N005	C008	C00H	109.76(15)
N006	Si03	C00K	112.69(9)	C00C	C008	C00D	111.46(17)
N006	Si03	C00M	112.20(9)	C00C	C008	C00H	108.49(16)
C00J	Si03	C00K	106.49(10)	C00D	C008	C00H	108.60(16)
C00J	Si03	C00M	105.40(12)	N004	C009	C00A	101.91(15)
C00K	Si03	C00M	106.61(12)	N005	C00A	C009	102.15(15)
C007	N004	C009	111.17(15)	N004	C00B	C00E	109.80(16)
C007	N004	C00B	124.43(15)	N004	C00B	C00L	109.64(16)
C009	N004	C00B	120.14(15)	N004	C00B	C00N	108.64(16)
C007	N005	C008	124.95(15)	C00E	C00B	C00L	110.90(17)
C007	N005	C00A	111.83(15)	C00E	C00B	C00N	107.75(18)
C00A	N005	C008	122.57(15)	C00L	C00B	C00N	110.06(19)
Si02	N006	Cu01	115.21(8)				

Table S7. Torsion angles for [Cu(^tBuNHC)(hmds)].

A	B	C	D	Angle/°	A	B	C	D	Angle/°
N004	C009	C00A	N005	-19.05(19)	C00A	N005	C008	C00C	122.52(18)
C007	N004	C009	C00A	19.0(2)	C00A	N005	C008	C00D	-115.31(19)
C007	N004	C00B	C00E	-54.6(2)	C00A	N005	C008	C00H	4.0(2)
C007	N004	C00B	C00L	67.5(2)	C00B	N004	C007	Cu01	10.7(3)
C007	N004	C00B	C00N	-172.20(19)	C00B	N004	C007	N005	-167.17(16)
C007	N005	C008	C00C	-67.5(2)	C00B	N004	C009	C00A	176.85(16)
C007	N005	C008	C00D	54.7(2)	C00F	Si02	N006	Cu01	36.83(12)

C007	N005	C008	C00H	174.00(17)	C00F	Si02	N006	Si03	-157.57(11)
C007	N005	C00A	C009	14.9(2)	C00G	Si02	N006	Cu01	156.81(10)
C008	N005	C007	Cu01	7.7(2)	C00G	Si02	N006	Si03	-37.59(15)
C008	N005	C007	N004	-174.33(16)	C00I	Si02	N006	Cu01	-83.29(11)
C008	N005	C00A	C009	-173.97(16)	C00I	Si02	N006	Si03	82.32(13)
C009	N004	C007	Cu01	167.40(13)	C00J	Si03	N006	Cu01	129.47(10)
C009	N004	C007	N005	-10.5(2)	C00J	Si03	N006	Si02	-35.82(15)
C009	N004	C00B	C00E	150.66(17)	C00K	Si03	N006	Cu01	-109.82(12)
C009	N004	C00B	C00L	-87.3(2)	C00K	Si03	N006	Si02	84.89(14)
C009	N004	C00B	C00N	33.1(2)	C00M	Si03	N006	Cu01	10.53(15)
C00A	N005	C007	Cu01	178.67(13)	C00M	Si03	N006	Si02	-154.77(13)
C00A	N005	C007	N004	-3.4(2)					

Table S8. Hydrogen atom coordinates ($\text{\AA} \times 10^4$) and isotropic displacement parameters ($\text{\AA}^2 \times 10^3$) for $[\text{Cu}(\text{tBuNHC})(\text{hmds})]$.

Atom	x	y	z	U(eq)
H00A	8664.82	9099.91	4286.01	31
H00B	8066.68	10461.33	4755.89	31
H00C	7049	10751.63	3295.26	33
H00D	8185.04	9813.53	2934.01	33
H00E	6186.9	6619.52	1168.96	42
H00F	4586.51	6470.91	382.51	42
H00G	4514	5976.04	1309.39	42
H00H	2748.53	7655.71	1653.06	46
H00I	2904.17	8288.89	788.27	46
H00J	3417.21	9365.55	1858.6	46
H00K	4158.7	8469.17	5177.21	44
H00L	4478.23	7231.86	5648.27	44
H00M	3783.87	6833.24	4510.83	44
H00N	4721.06	3769.61	1943.08	48
H00O	4075.86	2048.31	1455.89	48
H00P	4210.2	2748.43	2558.22	48
H00Q	567.49	1191.99	2141.94	45
H00R	758.38	437.19	1121.5	45
H00S	-624.23	1210.33	1181.62	45
H00T	6100.02	10336.72	1582.69	49
H00U	5505.31	9158.21	543.28	49
H00V	7113.21	9237.42	1296.59	49
H00W	327.18	3188.94	44.85	47
H00X	1514.79	2230.94	-154.39	47
H00Y	2153.59	3963.84	231.57	47
H00Z	-1607.65	4446.52	904.62	47
H	-2792.73	4269.95	1536.62	47
HA	-2055.9	2973.68	1167.73	47
H00	-699.31	2911.95	3266.47	54

HB	-1729.39	4020.66	3492.43	54
HC	93.22	4435.31	4092.48	54
H1	6046.1	5752.79	4248.3	55
HD	6772.17	6106.35	5379.88	55
HE	7837.76	6703.94	4771.27	55
H2	838.13	7289.12	3622.7	66
HF	-1011.57	6929.7	3099.31	66
HG	246.46	7320.39	2544.31	66
H3	8403	9269.24	5928.79	62
HH	7266.79	8667.28	6499.82	62
HI	6967.56	9937.99	6058.45	62

S6. Qualitative reactivity evaluation for $[\text{Cu}(\text{tBuNHC})(\text{hmds})]$

The high reactivity of the precursor was tested and confirmed qualitatively by exposing $[\text{Cu}(\text{tBuNHC})(\text{hmds})]$ to ambient, atmospheric conditions. A reaction with either oxygen or water in the air was visible after 1 min and indicated by a fast change from colorless to green, illustrating the overall high reactivity and instability towards oxygen or moisture.

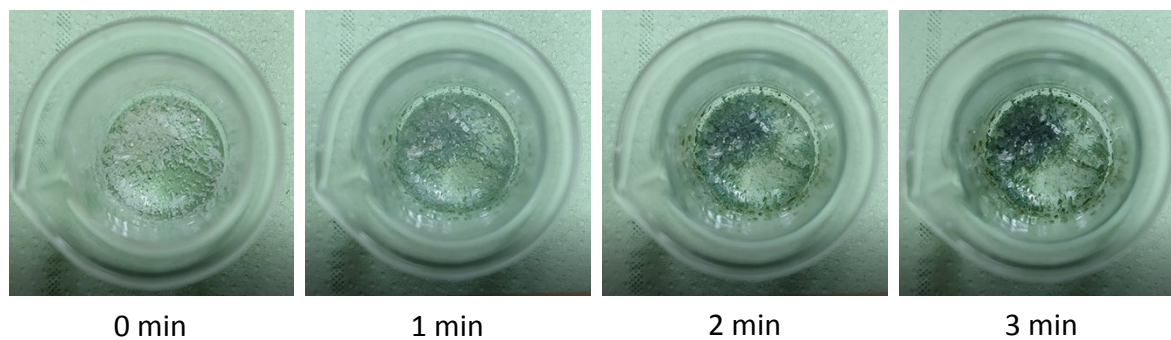


Figure S 3. Optical appearance of the precursor after a certain exposure to ambient air.

S7. Computational Method:

Density functional theory (DFT) was used to obtain the geometry and to simulate the reactivity of complexes. Precursor molecules and their ALD reaction products were modeled as isolated molecules in vacuum at zero Kelvin and zero GPa. Gas phase calculations were carried out using the TURBOMOLE suite of quantum chemical programs.¹¹ These calculations were performed by using the hybrid PBE0 functional, which incorporates 25% exact HF exchange,¹² and a polarized split valance basis set, denoted def-SV(P).¹³ An effective core potential is used for the Cu and Ag metal sites with 28 core electrons on Cu and 28 core electrons on Ag. A fine integration grid (m3) was used and the SCF convergence criterion was set to 10^{-6} Ha. Convergence criteria for the geometry was set to 10^{-3} Ha. The atomic structures of precursors are prepared from the experimental cif files in Accelrys Materials Studio 8.0 and are exported in xyz format. All atomic structures are available through a GitHub repository.¹⁹

The energy needed to lose the first ligand is calculated using:

$$E = (E_L + E_{P-1L}) - E_P \quad (1)$$

E_L – Computed total energy of one free ligand

E_P – Computed total energy of the precursor molecule

E_{P-1L} – Computed total energy of the precursor without the hmds ligand

For the example of $[Ag(tBuNHC)(hmds)]$:

$$E = [E_{hmds} + E_{Ag(tBuNHC)}] - E_{Ag(tBuNHC)(hmds)}$$

Interaction energies between precursors and H_2 molecules were calculated using:

$$E_{int} = \sum E_p - \sum E_r \quad (2)$$

E_p - Energy of products

E_r - Energy of reactants

For the example of the interaction of H_2 with $Ag(NHC)(hmds)$:

$$E_{int} = (E_{Ag(tBuNHC)-H} + E_{hmds-H}) - (E_{Ag(tBuNHC)(hmds)+H_2})$$

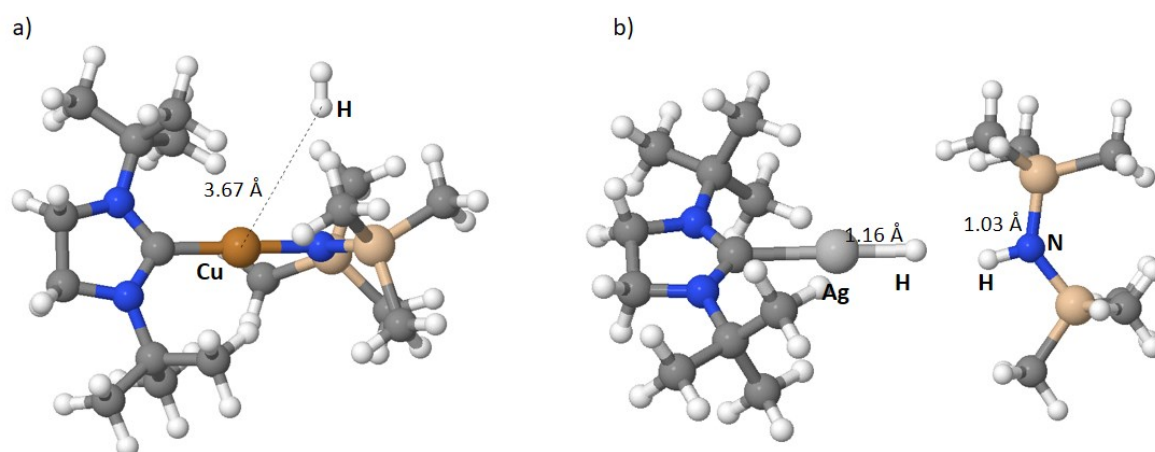


Figure S 4. Atomistic structures of (a) $[\text{Cu}(\text{tBuNHC})(\text{hmds})]$, (b) $[\text{Ag}(\text{tBuNHC})(\text{hmds})]$ after incorporating Hydrogen. Brown: Copper, Light grey: Silver, Blue: Nitrogen, Cream: Silicone, Dark grey: Carbon, White: Hydrogen.

Precursor models were developed to include the interaction with water molecules so the reactivity of precursors for experimental conditions could be investigated. Figure S7 shows the optimized structures of the precursors after the interaction with one water molecule. When one water molecule interacts with the $[\text{Cu}(\text{tBuNHC})(\text{hmds})]$ and $[\text{Ag}(\text{tBuNHC})(\text{hmds})]$ precursors, it preferably binds to the central metal atom and dissociates. For $[\text{Cu}(\text{tBuNHC})(\text{hmds})]$ the OH group of water binds to copper with a distance 1.98 Å and the remaining H atom binds to nitrogen with a distance 1.03 Å. In presence of water the Cu-N bond is lengthened from 1.88 Å to 2.18 Å. For $[\text{Ag}(\text{tBuNHC})(\text{hmds})]$ the OH group of water binds to silver with a distance 2.03 Å and the remaining H atom binds to nitrogen with a distance 1.05 Å. In presence of water the Ag-N bond breaks completely and the Ag-C bond is 1.08 Å

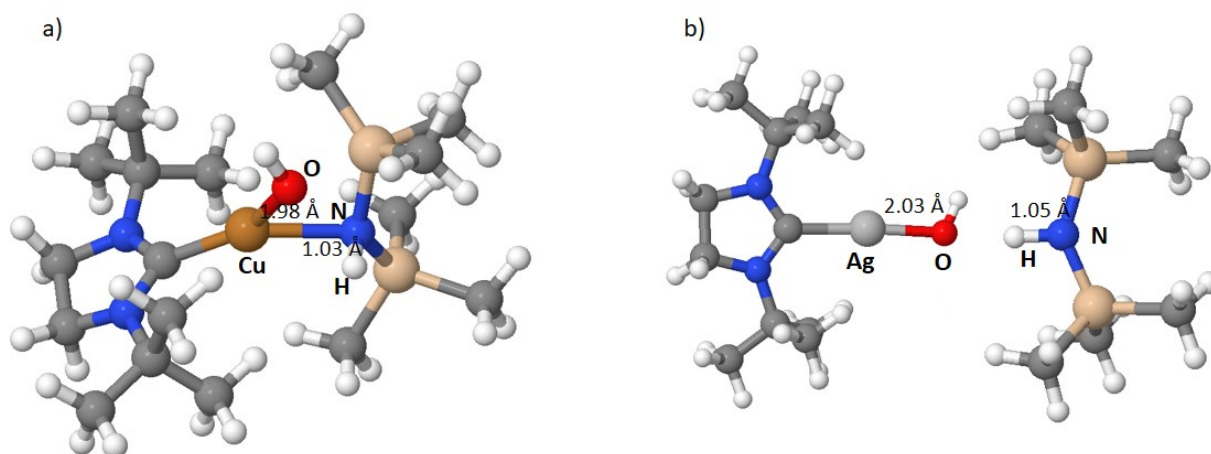


Figure S 5. Atomistic structures of (a) $[\text{Cu}(\text{tBuNHC})(\text{hmds})]$, (b) $[\text{Ag}(\text{tBuNHC})(\text{hmds})]$ after incorporating Oxygen. Colour code is the same as in figure S 4. Red: Oxygen.

S8. Thin film deposition and characterization

The deposition of the Cu films were performed in a home-built SALD system, described in detail previously.¹⁴ Throughout the experiments, borosilicate or silicon was used as substrates. Silicon substrates were only used for XPS analysis to ensure that the substrate was conductive enough for the analysis. Due to the fact, that our substrate contains SiO₂, we deposited 30nm SnO_x first and then we deposited our copper with APP-SALD. Thereby we wanted to avoid that XPS is used to measure the Si content of our substrate because our precursor contains Si and we would not distinguish between Si spectrum from substrate and precursor. The [Cu(^tBuNHC)(hmds)] precursor was kept in a precursor bubbler at 100 °C and a flow of 4 slm N₂ through the bubbler was used as carrier gas. Increasing the precursor temperature from 100 °C to 120 °C under identical experimental parameters did not lead to any notable change in the resulting GPC. For the growth of Ag layers, [Ag(^tBuNHC)(hmds)] was used at a bubbler temperature of 120°C. In all Cu and Ag experiments the substrate temperature was kept at 100°C. Hydrogen plasma with a mixture of 0.6 slm Ar / 0.6 slm H₂ as the working gas was used as the reducing agent and a dielectric barrier discharge (DBD) as the plasma source. A N₂ flow of 4 slm through each purge line was used as purge gas. The substrates are carried by a moving stage which is positioned roughly 200 μm below the reactor head and moved at a velocity of 5 mm/s. The film thickness was measured using a Dektak 150 stylus profiler. Scanning electron microscopy (SEM) investigations were carried out using a Philips XL30S FEG microscope with a field emission cathode. The SEM images were analyzed using the open source image analysis software FIJI.¹⁵ Rutherford backscattering spectrometry (RBS) was measured at the 4 MV tandem accelerator of the RUBION facility (Ruhr University Bochum, Germany) with a 2 MeV ⁴He⁺ ion beam (beam current of 20-40 nA) and a silicon surface barrier detector at an angle of 160°. X-ray photoelectron spectroscopy (XPS) was carried out at the chair of Experimentalphysik II (Ruhr University Bochum, Germany) with a VersaProbe 5000 spectrometer from PHI (Physical Electronics). An Al anode material with K_α radiation of 1486.7 eV and a spot size of 200 μm in diameter with a pass energy of 23.5 eV for high resolution measurements was used to guarantee an energy resolution of 0.05 eV. Sputtering was conducted with Ar⁺ ions at ion energies ranging from 500 eV to 1 keV with a 1x1 mm spot size and sputtering times of 4 minutes (500 eV) and 2 minutes (1 keV) respectively. The energy position of each spectrum was calibrated with respect to the signal of adventitious carbon on the non-sputtered surfaces. The main signal was set to 284.8 eV. The spectra were analyzed using Unifit 2017 developed by Unifit Scientific Software GmbH. Peak fitting was done after

subtraction of Shirley backgrounds and initial parameters for FWHM, peak separation and area ratios were set based on literature reports on XPS studies on copper. The AFM measurement of the deposited Cu layer was performed with a Burker Innova system in tapping mode and the electrical conductivity was measured using the van-der-Pauw method.

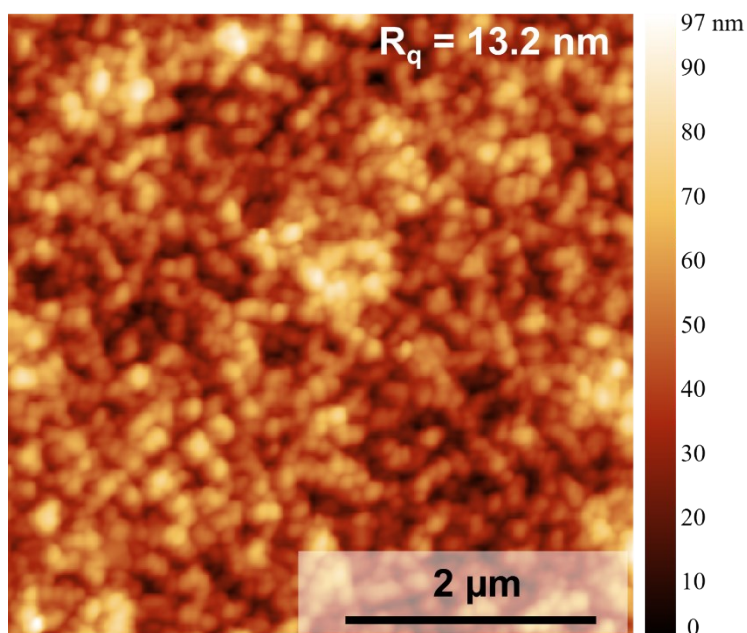


Figure S 6. AFM image of Cu layer grown by APP-ALD at 100 °C using 6000 cycles. Microscopy image is 5 x 5 μm²

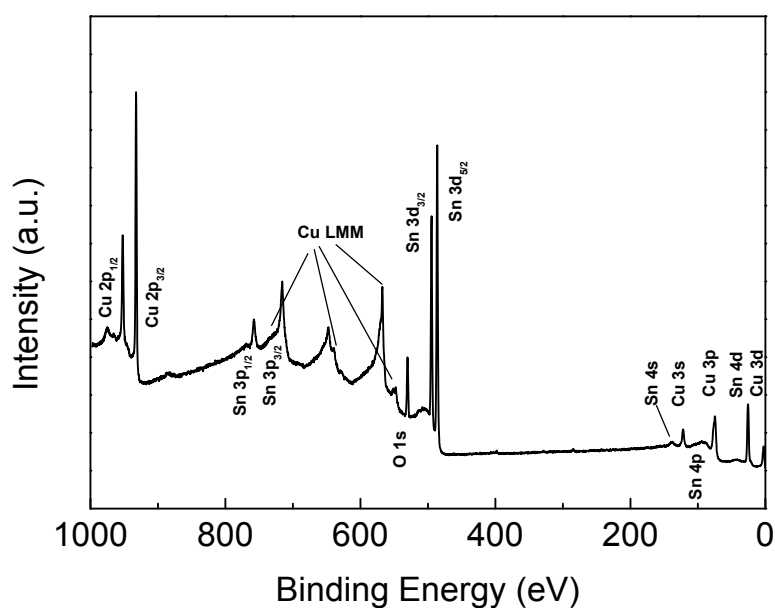


Figure S 7. XPS survey spectra of the Cu layer after 6 min sputtering at 1kV with Ar⁺ ions. For XPS we used conductive Si wafers as substrates. To entirely suppress the signal due to Si from the substrate, we coated 30 nm of SnO_x by ALD onto the substrate before we deposited the copper layer by APP-ALD.^{16,17}

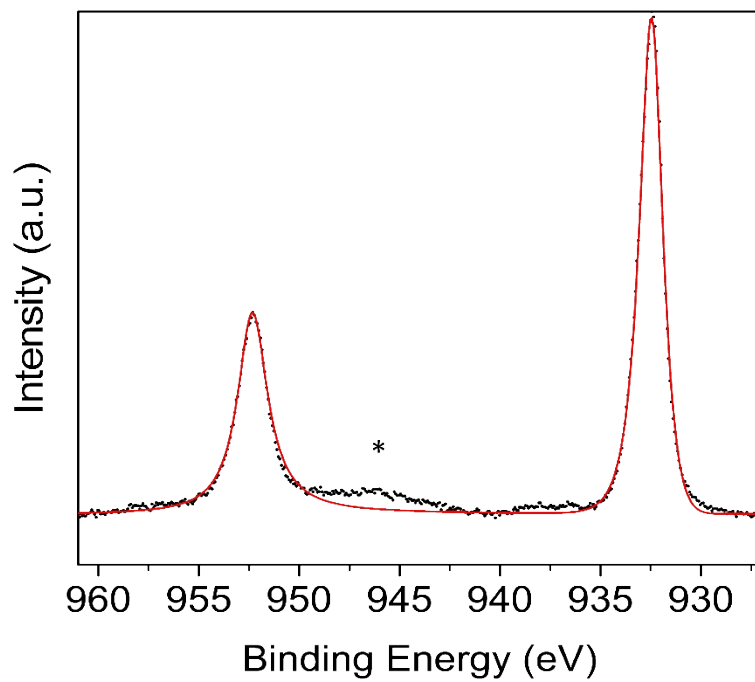


Figure S 8. XPS spectra of the core level spectra of Cu_{2p}. A satellite peak at around 945 eV (marked with an asterisk) indicates trace amounts of oxidized Cu (e.g. CuO).¹⁸

S9. References

- 1 O. V. Dolomanov, L. J. Bourhis, R. J. Gildea, J. A. K. Howard and H. Puschmann, *J. Appl. Crystallogr.*, 2009, **42**, 339–341.
- 2 G. M. Sheldrick, *Acta Crystallogr. Sect. C Struct. Chem.*, 2015, **71**, 3–8.
- 3 G. M. Sheldrick, *Acta Crystallogr. Sect. Found. Adv.*, 2015, **71**, 3–8.
- 4 P. Mårtensson and J.-O. Carlsson, *Chem. Vap. Depos.*, 1997, **3**, 45–50.
- 5 A. Niskanen, A. Rahtu, T. Sajavaara, K. Arstila, M. Ritala and M. Leskelä, *J. Electrochem. Soc.*, 2005, **152**, G25.
- 6 L. Wu and E. Eisenbraun, *J. Vac. Sci. Technol. B Microelectron. Nanometer Struct.*, 2007, **25**, 2581.
- 7 C. Jezewski, W. A. Lanford, C. J. Wiegand, J. P. Singh, P.-I. Wang, J. J. Senkevich and T.-M. Lu, *J. Electrochem. Soc.*, 2005, **152**, C60.
- 8 D.-Y. Moon, W.-S. Kim, T.-S. Kim, B.-W. Kang, J.-W. Park, S. J. Yeom and J. H. Kim, *J. Korean Phys. Soc.*, 2009, **54**, 1330–1333.
- 9 Z. Guo, H. Li, Q. Chen, L. Sang, L. Yang, Z. Liu and X. Wang, *Chem. Mater.*, 2015, **27**, 5988–5996.
- 10 J. P. Coyle, G. Dey, E. R. Sirianni, M. L. Kemell, G. P. A. Yap, M. Ritala, M. Leskelä, S. D. Elliott and S. T. Barry, *Chem. Mater.*, 2013, **25**, 1132–1138.
- 11 R. Ahlrichs, M. Bär, M. Häser, H. Horn and C. Kölmel, *Chem. Phys. Lett.*, 1989, **162**, 165–169.
- 12 J. P. Perdew, K. Burke and M. Ernzerhof, *Phys. Rev. Lett.*, 1996, **77**, 3865–3868.
- 13 A. Schäfer, H. Horn and R. Ahlrichs, *J. Chem. Phys.*, 1992, **97**, 2571–2577.
- 14 L. Hoffmann, D. Theirich, S. Pack, F. Kocak, D. Schlamm, T. Hasselmann, H. Fahl, A. Raupke, H. Gargouri and T. Riedl, *ACS Appl. Mater. Interfaces*, 2017, **9**, 4171–4176.
- 15 J. Schindelin, I. Arganda-Carreras, E. Frise, V. Kaynig, M. Longair, T. Pietzsch, S. Preibisch, C. Rueden, S. Saalfeld, B. Schmid, J. Y. Tinevez, D. J. White, V. Hartenstein, K. Eliceiri, P. Tomancak and A. Cardona, *Nat. Methods*, 2012, **9**, 676–682.
- 16 S. Trost, A. Behrendt, T. Becker, A. Polywka, P. Görrn and T. Riedl, *Adv. Energy Mater.*, 2015, **5**, 1500277.
- 17 A. Behrendt, C. Friedenberger, T. Gahlmann, S. Trost, T. Becker, K. Zilberberg, A. Polywka, P. Görrn and T. Riedl, *Adv. Mater.*, 2015, **27**, 5961–5967.
- 18 M. C. Biesinger, L. W. M. Lau, A. R. Gerson and R. St. C. Smart, *Appl. Surf. Sci.*, 2010, **257**, 887–898.
- 19 https://github.com/ArbreshaMuriqi/Ag-Cu_Precursors.